PHYSICAL REVIEW E VOLUME 52, NUMBER 3 SEPTEMBER 1995

# Double layer relaxation at rough electrodes

Amy E. Larsen and David G. Grier
*The James Franck Institute, The University of Chicago, 5640 S. Ellis Avenue, Chicago, Illinois 60637*

Thomas C. Halsey
*Exxon Research & Engineering, Route 22E, Clinton Township, Annandale, New Jersey 08801*

(Received 4 November 1994)

We describe measurements of the complex admittance of the interface between electrodeposited fractal electrodes and electrolytic solutions over the frequency range 100 Hz to 100 kHz. Scaling with a single size-dependent frequency collapses these data onto a universal curve. This scaling collapse provides quantitative support for the Halsey-Leibig theory for constant phase angle behavior and a technique for measuring the multifractal descriptors $D_f$ and $\tau(2)$ for such electrodes. [$D_f$ is the rough electrode's fractal dimension, and the multifractal exponent $\tau(2)$ is the correlation dimension of the surface's harmonic measure.]

PACS number(s): 68.70.+w, 73.25.+i, 61.43.Hv

The electrical impedance of electrode-electrolyte interfaces is often observed to have a component which scales nontrivially with frequency:

$$Z(\omega) \propto (i\omega)^{-\beta} \tag{1}$$

over at least some range of frequencies, $\omega$. This phenomenon, referred to as a constant phase angle (CPA) element, was reported by Wolff [1] in 1926. The possibility that interfacial roughness might induce CPA behavior was suggested a quarter century later [2] but was not emphasized until some years after that [3–5]. In the decade since the pioneering effort of Le Mehaute and Crepy [6] to explain CPA scaling in terms of the fractal structure of rough electrodes, several competing theories have been proffered [7]. The majority of these treat the fractal surface as a blocking electrode, one at which no electrochemical reactions occur and which, therefore, admits no faradaic current. The theory of Halsey and Leibig (HL) [8] differs from the earlier studies in asserting that the electrodes' multifractal nature induces this behavior through the relation

$$\beta = \frac{\tau(2) - d + 2}{D_f - d + 2}. \tag{2}$$

Here $D_f$ is the rough electrode's fractal dimension, and $d$ is the dimension of the embedding space. The multifractal exponent $\tau(2)$ is the correlation dimension of the surface's harmonic measure [9]. Recent simulations on fractal Koch curves embedded in two dimensions agree well with this prediction [10] and are not consistent with other predicted forms for $\beta$.

We describe *in situ* measurements of the frequency-dependent admittance of well-characterized fractal electrodes grown by electrochemical deposition. We observe CPA behavior at high frequencies and are able to collapse a wide range of data onto a universal curve by scaling with a single characteristic frequency which in turn scales with system size. The success of this scaling collapse supports the assumptions underlying the HL theory; the extracted scaling exponents also are consistent with its results summarized in Eq. (2). In contrast to the results of Pajkossy [11], our observations are consistent with a geometric origin for CPA scaling for this system. While our results are reproducible from run to run, the following discussion focuses on a typical data set for clarity.

We prepare fractal electrodes in the manner described by Brady and Ball [12]. As shown schematically in Fig. 1, copper is electrodeposited onto the freshly cut tip of an otherwise insulated wire 25 $\mu$m in diameter from an aqueous solution containing 0.01$M$ $CuSO_4$. The electrolyte fills a rectangular glass cell and wets a coil of 22 gauge copper wire 1 cm in diameter with a pitch of roughly 1 mm. This coil serves as the anode in the electrochemical cell. Its open structure permits direct observation of the electrodeposition process. The fine wire tip, which serves as the cathode, is centered within the coil using a micropositioner. When a constant voltage is applied across this system, copper ions in solution deposit onto the cathode wire and form an aggregate. We apply $-0.5$V to the cathode and hold the anode at virtual ground. An excess of supporting electrolyte (0.10$M$ $Na_2SO_4$) screens out electric fields in the solution, so that transport of copper ions to the growth front is limited by

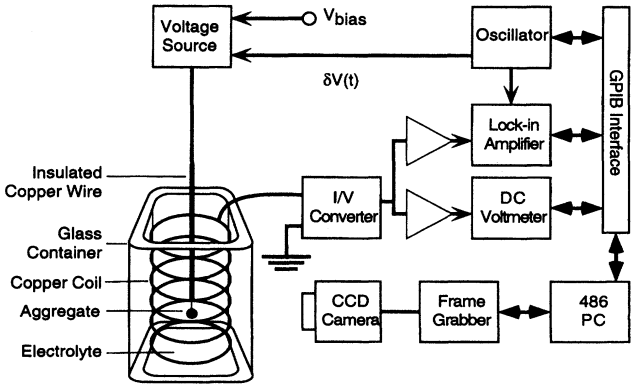


FIG. 1. Schematic diagram of experimental system. Vibration isolation, temperature control, and gas handling systems are not shown for clarity.

 

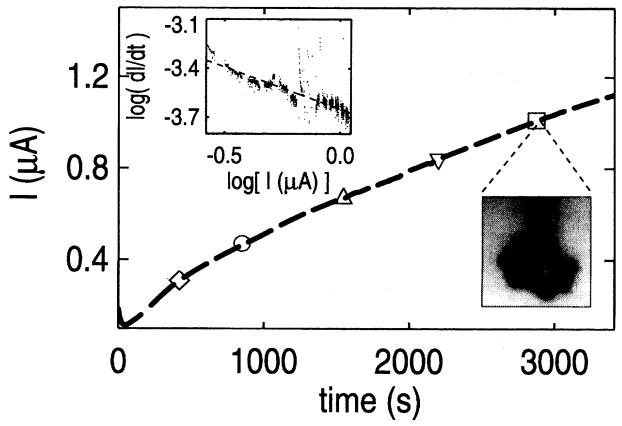


FIG. 2. Deposition current as a function of time. Symbols indicate times of admittance spectrum measurements shown in Fig. 3. Upper inset: Fractal scaling according to Eq. (3). The dashed line is a least squares best fit whose slope indicates a fractal dimension of $D_f = 2.55 \pm 0.05$. Lower inset: Typical aggregate approximately 100 $\mu$m in diameter.

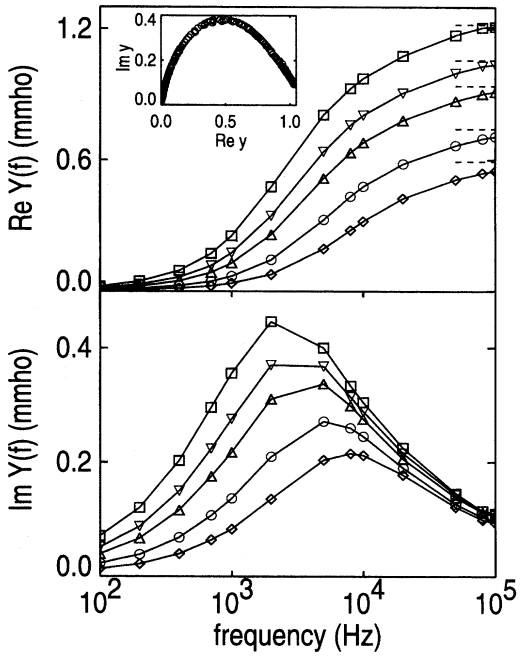


FIG. 3. (Top) The real admittance as a function of frequency. The plot symbols correspond to the times shown in Fig. 2. Extrapolated values for $Y_0$ appear as dashed lines. Inset: Re $y(\omega)$ versus Im $y(\omega)$. (Bottom) The imaginary admittance as a function of frequency. CPA scaling is observed on the high frequency side of the absorption peak.

diffusion. The solution is acidified to $p$H 4 with added $H_2SO_4$ and is deoxygenated by bubbling with argon before being added to the deposition cell. These precautions minimize the oxidation rate of freshly deposited copper. The free length of the cathode wire is kept below 5 mm to minimize mechanical instabilities. We also add a chemically inert gel [agarose (0.5 g/100 ml)] to mechanically stabilize the electrolyte against convection. Finally, the entire growth cell is vibrationally isolated, maintained at a temperature constant to within 0.1 °C, and situated in a water-saturated argon atmosphere.

The growth conditions in this system resemble very closely the diffusion-limited aggregation (DLA) model [13,12] in which fractal branched structures grow by the sequential accretion of random walkers. While the *a priori* theory of DLA is not yet complete, extensive numerical simulations reproducibly generate three dimensional clusters with multifractal descriptors $D_f = 2.51 \pm 0.06$ [14] and $\tau(2) = 1.82 \pm 0.02$ [15]. The HL theory thus predicts $\beta = 0.54 \pm 0.03$ for DLA-like electrodes.

We monitor an electrodeposit's geometry as it grows both by direct observation and also by measuring the deposition current. An aggregate such as the example inset in Fig. 2 reaches a diameter of 100 $\mu$m in about one hour. Following Brady and Ball [12], we treat the aggregate as having an effective spherical radius, $r$, proportional to its radius of gyration. The diffusion-limited deposition current arriving at the surface of a sphere is proportional to its radius [16], $I(r) \propto r$, and should be independent of the applied voltage. Carro *et al.* [17] have confirmed that the deposition current for electrodeposited clusters is proportional to their apparent radii. The very small response in the deposition current to low frequency voltage perturbations (see Fig. 3) is consistent with diffusive transport. The aggregate's mass scales with the effective radius and is proportional to the total charge deposited: $M(r(t)) \propto \int_0^t I(t)dt$, so that $I^{D_f}(t) \propto \int_0^t I(t)dt$. Recasting this as a derivative relation:

$$\frac{\partial I}{\partial t} \propto I^{2-D_f}, \tag{3}$$

avoids complications due to initial conditions. The fractal dimension then emerges from the slope of the log-log plot of Eq. (3), as shown in the inset to Fig. 2.

As in previous studies [12,17], the range of measurable scaling in current, and thus of radius, covers less than one decade. Ordinarily, such scaling plots should be treated with extreme skepticism. However, the lower limit of the scaling domain is set by the 25 $\mu$m diameter of the cathode and not by the smallest feature size of the electrodeposit. Scanning electron micrographs reveal structures as small as 100 nm. While such features are masked by the dimensions of the wire in Fig. 2, their appearance means that structure in the disordered branches extends over three decades in linear dimension. The value $D_f = 2.55 \pm 0.05$ extracted for a series of aggregates grown under similar conditions is consistent with results of the DLA model and suggests that self-similarity also might extend over three decades.

The frequency-dependent contribution of a fractal blocking electrode to the overall system impedance arises from the effective capacitance of the electrode-electrolyte interface. For the geometry of our experiment, this contribution appears in series with the resistance of the electrolyte and in parallel with the comparatively small capacitance of the rest of the cell. Due to stray reactance in series with the electrochemical cell, it is most convenient to study the complex admittance, $Y(\omega) = 1/Z(\omega)$.

The range of frequencies over which we expect to see CPA scaling is limited by the size of the aggregate at low frequencies and by the smallest feature size at high frequencies. For an isolated 100 $\mu$m diameter aggregate with 100 nm features, HL [8] suggest that CPA scaling should be observed between 10 Hz and 1 MHz. Cao *et al.* [10] point out that this range will be restricted by the cell capacitance to between 500 Hz and 500 kHz for our system. Following the HL theory, we expect to see CPA scaling above the absorption peak in $Y(\omega)$. This is confirmed by our results below.

We measure the frequency dependence of the system's complex admittance at regular intervals during an aggregate's growth by superimposing a 1.6 mV p.p. sinusoidal perturbation over the 0.5 V deposition voltage. The sequence of perturbing signals in a single spectrum includes 13 frequencies ranging between 100 Hz and 100 kHz. The duration of each spectral measurement is indicated by the gaps in the current trace in Fig. 2. The system's response is measured with a precision wide-bandwidth current-to-voltage converter whose output is buffered before measurement with a lock-in amplifier referenced to the perturbation signal. The overall performance of this system is calibrated with networks of resistors and capacitors chosen to mimic the characteristics of the electrochemical cell. At the highest frequency of this study, 100 kHz, the phase accuracy of the measurement system is found to be better than 1° while the amplitude resolution is better than 50 nA. At lower frequencies, the performance is considerably better. The main advantage of our approach is that while the response of the cell is diffusion limited at the low frequencies on which the electrodeposition takes place, the high frequency behavior is that of a linear electrical system.

The real and imaginary parts of the admittance at several stages in a typical aggregate's growth appear in Fig. 3 with plot symbols corresponding to those in Fig. 2. To compare our results with theoretical predictions we define the dimensionless complex admittance $y(\omega)=Y(\omega)/Y_0$, where $Y_0$ is the high frequency limit of the real admittance which arises from the conductance of the electrolyte bounding the aggregate. We estimate $Y_0$ by extrapolating from curves such as those in Fig. 3 under the assumption that $Y_0 \propto r^{\gamma}$. For $\gamma=0.94\pm0.01$ the real and imaginary parts of $y(\omega)$ fall on the single smooth curve shown as the inset to Fig. 3. Estimated values of $Y_0(r)$ appear as dashed lines in Fig. 3. The low frequency limit of the real admittance is a measure of the faradaic contribution to the electrode's transport properties. From Figs. 2 and 3, we estimate this conductance to be smaller than $10^{-3}$ mmho which is more than two orders of magnitude smaller than the high frequency admittance. To this extent, our aggregates act as blocking electrodes in the frequency range of interest.

In addition to this conventional static scaling, which corrects for the size dependence of the overall magnitude of the admittance, we examine size-dependent scaling in the dynamical response. Without reference to any particular model, we assume a scaling form for the dimensionless normalized admittance:

$$y(\omega)-1=f\left(\frac{\omega}{\omega_c}\right), \tag{4}$$

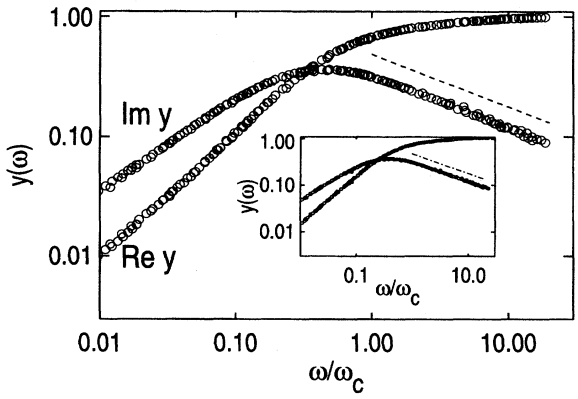


FIG. 4. Dimensionless complex admittance as a function of rescaled frequency for one aggregate at 12 different sizes. The dashed line is a fit to the high-frequency exponential tail for scaled frequencies greater than 1. The line is offset upward for clarity. Its slope gives the CPA exponent $\beta=0.43\pm0.03$. Inset: Scaled complex admittance data for another aggregate: $D_f=2.52\pm0.05$, $\alpha=1.52\pm0.08$, $\beta=0.41\pm0.03$.

where the function $f(x)$ is, as yet, undetermined. The strongest assumption in Eq. (4) is that the admittance scales with a single characteristic frequency, $\omega_c$. This differs diametrically from models which introduce a range of relaxation rates to account for surface inhomogeneity [11]. If we further assume that the characteristic frequency, $\omega_c$, scales with the size of the aggregate, $\omega_c \propto r^{-\alpha}$, and recall that the aggregate's size is proportional to the deposition current, we find

$$\omega_c=\omega_o\left(\frac{I}{I_o}\right)^{-\alpha}, \tag{5}$$

where $I_o \approx 1$ nA is a characteristic current scale [12] corresponding to the observed typical crystallite size of 100 nm and $\omega_o=(9\times10^{11}\ \text{sec}^{-1}\ \Omega\ \text{cm})\ \sigma_e/\epsilon=9\times10^8$ rad/s is a characteristic frequency [8] for an electrolyte of resistivity $\sigma_e^{-1}\approx 10^2\ \Omega$ cm, and dielectric constant $\epsilon\approx10$.

If Eqs. (4) and (5) reflect the dynamics adequately, then we expect to find values of $\alpha$ for which all the admittance data for a given aggregate at different sizes collapse onto a single universal curve. Figure 4 shows the real and imaginary parts of the rescaled admittance data for the aggregate in Fig. 1 at 12 different stages of its growth collapsed according to Eqs. (4) and (5) with $\alpha=1.47\pm0.08$. The success of this scaling collapse justifies our assumptions that the dynamical response is characterized by a single frequency which in turn scales with system size and is the central experimental observation of this paper.

If we now assume CPA scaling, $f(x)\propto x^{-\beta}$, for $\omega/\omega_c>1$ we then obtain a new expression for the imaginary part of the dimensionless admittance:

$$\text{Im}\ y(\omega)\propto\left(\frac{I}{I_o}\right)^{-\alpha\beta}\left(\frac{\omega}{\omega_o}\right)^{-\beta}, \tag{6}$$

from which we can extract the CPA exponent $\beta$. Multiplying Im $y(\omega)$ by the dimensional factor $Y_0/\omega$ gives a typical scale of nanofarads for the interfacial capacitance. The slope

of the dashed line in Fig. 4 indicates $\beta = 0.43 \pm 0.03$. Comparable CPA exponents are extracted from each of the spectra at different sizes individually. These measurements and similar results for other aggregates (see, for example, the inset to Fig. 4) are not consistent with the scaling hypothesis $\beta = (D_f - 1)^{-1}$ claimed in other studies on model fractal electrodes [18,19].

The same assumptions which are supported by the successful collapse of the admittance data also underlie the HL theory for CPA scaling. Their result for the dimensionless admittance:

$$y(\omega) \approx 1 + \frac{g}{\beta}\left(\frac{\omega_o}{i\omega}\right)^{\beta}, \tag{7}$$

where $g \propto r^{d-2-\tau(2)}$, reflects these assumptions and suggests an overall scaling form

$$\text{Im } y(\omega) \propto l^{d-2-\tau(2)} \omega^{-\beta}. \tag{8}$$

Comparing Eq. (8) and the HL result in Eq. (2) with the experimentally observed scaling form in Eq. (6) gives

$$\alpha = D_f - 1 \tag{9}$$

in $d = 3$ dimensions. Equation (9) can also be derived from the scaling form given in Eq. (4) if we assume low frequency capacitive behavior, with the capacitance proportional to the surface area of the fractal electrodeposit. The data collapse in Fig. 4 thus provides an independent measure of the fractal dimension, $D_f = 2.47 \pm 0.08$, whose agreement both with the value found from current scaling and also with the accepted value for DLA provides additional quantitative support for the HL theory.

Equations (2), (8), and (9) enable us to extract the multifractal descriptor $\tau(2) = \alpha\beta + 1$ from our scaling data. The result, $\tau(2) = 1.63 \pm 0.06$, is roughly 10% smaller than the presently accepted value for DLA. This small but real discrepancy may arise from a systematic error in calculating this numerical value from simulation data or from subtleties in the electrodeposition process that lower $\tau(2)$ in the physical system with respect to its DLA value. If the latter is the case, then the impedance method allows us to distinguish electrodeposits from DLA clusters despite their identical fractal dimensions.

We would like to acknowledge the donors of the Petroleum Research Fund of the American Chemical Society for supporting this research.

[1] I. Wolff, Phys. Rev. **27**, 755 (1926).
[2] R. de Levie, Electrochim. Acta **10,** 113 (1965).
[3] W. Scheider, J. Phys. Chem. **79**, 127 (1975).
[4] R. D. Armstrong and R. A. Burnham, J. Electroanal. Chem. **72,** 257 (1976).
[5] P. H. Bottelberghs and G. H. J. Broers, J. Electroanal. Chem. **67,** 155 (1976).
[6] A. Le Mehaute and G. Crepy, Solid State Ionics **9 & 10,** 17 (1983).
[7] P. G. de Gennes, C. R. Acad. Sci. Paris **295,** 1061 (1982); S. H. Liu, Phys. Rev. Lett. **55,** 529 (1985); T. Kaplan, L. J. Gray, and S. H. Liu, Phys. Rev. B **35,** 5379 (1987); L. Nyikos and T. Pajkossy, Electrochim. Acta **30,** 1533 (1985); J. C. Wang, *ibid.* **33,** 707 (1988); T. C. Halsey, Phys. Rev. A **36,** 5877 (1987); **35,** 3512 (1987); R. Ball and M. Blunt, J. Phys. A **21,** 197 (1988); L. Nyikos and T. Pajkossy, Electrochim. Acta **31**, 1347 (1986); B. Sapoval, J. N. Chazalviel, and J. Peyriere, Phys. Rev. A **38**, 5867 (1988).
[8] T. C. Halsey and M. Leibig, Ann. of Phys. **219,** 109 (1992); Phys. Rev. A **43,** 7087 (1991).
[9] T. C. Halsey, M. H. Hensen, L. P. Kadanoff, I. Procaccia, and B. I. Shraiman, Phys. Rev. A **33,** 1141 (1986).
[10] Q.-z. Cao, P.-z. Wong, and L. M. Schwartz (private communication).
[11] T. Pajkossy, J. Electroanal. Chem. **364**, 111 (1994).
[12] R. M. Brady and R. C. Ball, Nature (London) **309**, 225 (1984).
[13] T. A. Witten, Jr. and L. M. Sander, Phys. Rev. Lett. **47,** 1400 (1981); T. A. Witten and L. M. Sander, Phys. Rev. B **27,** 5686 (1983).
[14] P. Meakin, Phys. Rev. A **27**, 604 (1983).
[15] M. Leibig and T. C. Halsey, J. Electroanal. Chem. **358,** 77 (1993).
[16] M. von Smoluchovski, Phys. Z. **17,** 557 (1916); M. von Smoluchovski, Z. Phys. Chem. **92,** 129 (1917).
[17] P. Carro, S. L. Marchiano, A. Hernandez Creus, S. Gonzalez, and A. J. Arvia, Phys. Rev. E **48**, R2374 (1993).
[18] A. Hernandez Creus, A. E. Bolzan, P. Carro, S. Gonzalez, R. C. Salvarezza, and A. J. Arvia, Electrochim. Acta **38,** 1545 (1993).
[19] B. Sapoval, R. Gutfraind, P. Meakin, M. Keddam, and H. Takenouti, Phys. Rev. E **48**, 3333 (1993).

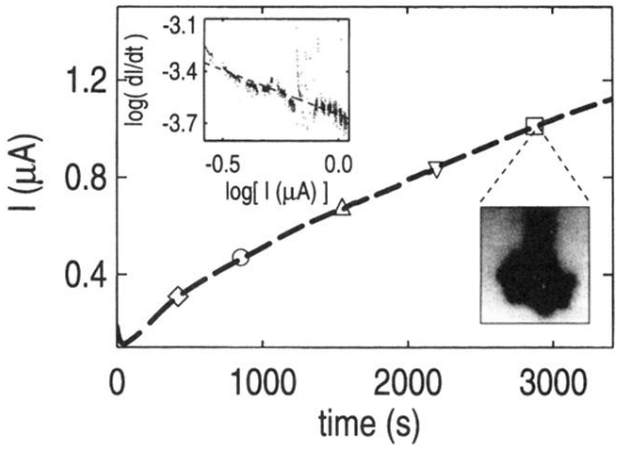


FIG. 2. Deposition current as a function of time. Symbols indicate times of admittance spectrum measurements shown in Fig. 3. Upper inset: Fractal scaling according to Eq. (3). The dashed line is a least squares best fit whose slope indicates a fractal dimension of $D_f = 2.55 \pm 0.05$. Lower inset: Typical aggregate approximately 100 $\mu$m in diameter.